Crosstalk Statistics via Collocation Method

Original
Crosstalk Statistics via Collocation Method / Diouf, F.; Canavero, Flavio. - STAMPA. - (2009), pp. 92-97. (Intervento presentato al convegno 2009 IEEE International Symposium on EMC tenutosi a Austin, TX (USA) nel Aug.17-21, 2009) [10.1109/ISEMC.2009.5284686].

Availability:
This version is available at: 11583/2279574 since:

Publisher:
IEEE

Published
DOI:10.1109/ISEMC.2009.5284686

800G intra-data center transceiver requirements for SWDM VCSEL-MMF links

Ann Margareth Rosa Brusin
Politecnico di Torino, DET
Torino, Italy
ann.rosabrusin@polito.it

Fabrizio Forghieri
Cisco Photonics srl
Vimercate, Italy
fforghie@cisco.com

Andrea Carena
Politecnico di Torino, DET
Torino, Italy
andrea.carena@polito.it

***Abstract*—To cope with AI growth, future data-centers will require 800G interconnections: low cost VCSEL-MMF solutions deployed in the 4λ-SWDM are a viable approach thanks to improvements in device technology. We analyzed PAM-M based implementations defining bandwidth and noise requirements.**

***Index Terms*—Short wavelength division multiplexing, vertical cavity surface emitting laser, multi-mode fibers.**

I. Introduction

In inter-data centers short link connections mainly rely on vertical cavity surface emitting lasers (VCSELs) and multi-mode fibers (MMFs), because of the reduced costs and the easier laser-fiber coupling. State-of-the-art devices can operate up to 100 Gbps per lane (λ) using standard pulse amplitude modulation (PAM)-4 [1]. According to the guidelines indicated by the IEEE P802.3db Short Reach Fiber Task Force and the IEEE P802.3dj Ethernet Task Force, 4λs short wavelength division multiplexing (SWDM) solutions can be exploited to enable 400G links. However, the recent spread of artificial intelligence on general public applications is causing an unprecedented increase of connections requiring high throughput up to 800G net bit rate (200 Gbps per lane). As a matter of fact, the move towards 800G solutions has already started [2], but further studies are necessary.

Besides the impact of modal and chromatic dispersion that limits the system maximum reach [3], [4], the main challenge to transmit at such higher bit rates is represented by the developement of novel VCSEL sources and transimpedance amplifiers (TIA) with larger bandwidths and lower noise levels: the relative intensity noise (RIN) for the VCSEL and the input referred noise density (IRND) for the TIA. Research trends are going towards these directions, with already promising results [5]–[7]. However, the articles and the conference proceedings that can be found in the literature on 200 Gbps transmissions usually present new or improved technology (larger bandwidth and lower noise levels) for the transceiver (TRX), but tested just for specific conditions and for a limited number of links. Unlike single mode fiber-based links, multi-mode interconnections relying on VCSELs and MMF are characterized by a large variability in performance and reach, mainly due to differences in the MMF fabrication and in the mode coupling with VCSELs. Therefore, given the statistical nature of VCSEL+MMF links, an analysis on few cases is not exhaustive to define the performance of a multi-mode system, which indeed should be evaluated on a large set of links. At the same time, also the definition of the TRX requirements should be defined accounting for the statistical behavior of VCSEL+MMF links.

This is the target of the paper: through time-domain simulations, we carry out an extensive study to assess the requirements for this new generation of devices. Starting from the scenario analyzed in [4], which considered a 4λs PAM-4 SWDM system with 100 Gbps per lane and a large set of VCSEL+MMF links, we define bandwidth and noise requirements for both transmitter (TX) and receiver (RX) operating at the more challenging 200 Gbps per lane net bit rate. The analysis is extended also to other modulation formats: PAM-6 and PAM-8.

II. Description of the Simulation Setup

The scheme of the simulation setup is shown in Fig. 1. As mentioned in the Introduction, transmissions at higher bit rates are limited by the bandwidth of the devices used to implement the TX and the RX sides. Specifically, the TX available bandwidth ($\mathrm{B_{TX}}$) is limited by the -3 dB bandwidth of the VCSEL transfer function $\mathrm{H_{VCSEL}}(f)$. Instead, at the RX side, two devices are actually responsible of limiting the available bandwidth: the photodiode (PIN) and the TIA. For simplicity, we consider the -3 dB bandwidth ($\mathrm{B_{RX}}$) of the overall transfer function $\mathrm{H_{PIN+TIA}}(f)$ given by the cascade of these two devices. The photodiode responsivity R is set to 0.5 A/W.

In the simulator, to account for the noise generated by the devices, two blocks are included in order to add the RIN of the VCSEL and the thermal noise of the TIA (governed by the IRND). The shot noise is also included, but its impact is negligible.

The study is performed for different scenarios through time-domain simulations using a simulator developed in-house. We assume a SWDM system with the four wavelengths at 850 nm, 880 nm, 910 nm and 940 nm, targeting 30 m distance. In [4], a large dataset of VCSEL+MMF links (OM3 and OM4) was considered to account for the statistical variability of the link.

This work was supported by the Cisco Sponsored Research Agreement "RISE-ONE 2024" and by the PhotoNext Center of Politecnico di Torino.

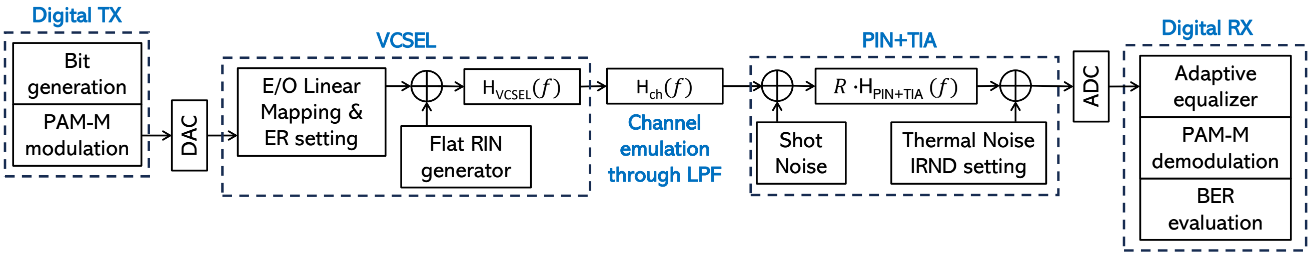

Fig. 1. Simulation setup. DAC: digital-to-analog converter, RIN: relative intensity noise, LPF: low-pass filter, R: photodiode responsivity, IRND: input referred noise density, ADC: analog-to-digital converter, BER: bit error rate.

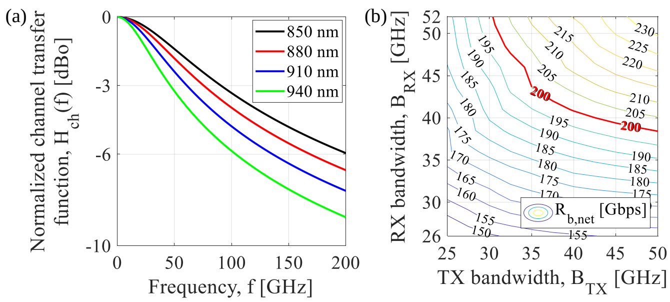

Fig. 2. (a) Normalized channel transfer functions at 30 m for the different SWDM wavelengths generated through a single pole LPF with cut-off frequencies corresponding to the bandwidths guaranteed by the 99% of the links of OM4 fibers dataset analyzed in [4]. (b) Net bit rate ($R_{b,net}$) at target BER as a function of the TRX bandwidths at 940 nm for PAM-4 transmitting over 30 m and using MLSE in case of RIN=-145 dBe/Hz and IRND=14.1 pA/$\sqrt{\text{Hz}}$.

However, the optimization of the TRX parameters for a statistically varying channel is unpractical from a computational point of view.

To simplify the analysis, we reduce the wide variability of the link by emulating the MMF channel through a single pole low pass filter (LPF). The cut-off frequency of the filter is defined by the bandwidth guaranteed by the 99% of the OM4 links of the dataset analyzed in [4]. The resulting bandwidths for the target distance of 30 m are 90.9 GHz, 75.7 GHz, 61.1 GHz and 46.5 GHz, respectively at 850 nm, 880 nm, 910 nm and 940 nm. We do not consider OM3 fibers at 200 Gbps since the reachable distances are further reduced due to the stronger modal dispersion. This approach, based on the MMF channel emulation through a LPF, allows to reduce the computational time by a factor of $\sim 10^4$ for the OM4 case.

Fig. 2(a) reports the normalized channel transfer functions $\mathrm{H_{ch}(f)}$ generated as described above for the four wavelengths of the SWDM system. As also shown in [4], from there we can see that the band limitation effect induced by the MMF channel is stronger at 940 nm, which indeed is the channel limiting the overall SWDM performance. For this reason, we focus our analysis at this wavelength only.

Besides PAM-4, we also test other modulation formats: standard PAM-8 and PAM-6 as described in [8]. Enhanced forward error correction (E-FEC) code is considered, with 4×10^{-3} target bit error rate ($\mathrm{BER_T}$) and 10.35% FEC overhead. This means that for 200 Gbps net rate, the actual transmitted gross rate is 220.7 Gbps.

Adaptive equalization is implemented to recover for channel impairments and bandwidth limitation effects. In particular, the feed-forward equalizer (FFE) and the maximum likelihood sequence estimation equalizer (MLSE) are used. To measure the system performance, the simulator outputs the bit error rate (BER) evaluated through error counting.

III. Analysis of Transceiver Bandwidth and Noise Requirements

We start our analysis considering RIN=-145 dBe/Hz and IRND=14.1 pA/$\sqrt{\text{Hz}}$, values that are technologically feasible [5], [7]. Fig. 2(b) shows the contour plot of the maximum achievable net bit rate as a function of the TX and RX bandwidths in case of PAM-4 and MLSE. The TX and RX bandwidths are in the range [25,50] GHz and [26,52] GHz, respectively, where 25 GHz and 26 GHz are the values considered in [4] for 400G (100G lambda) solutions. In red we highlight the iso-curve related to the target 200 Gbps: moving on this curve it is possible to determine the set of TX and RX bandwidths delivering the desired throughput. Repeating the same study for PAM-6 and PAM-8 and extracting the iso-curve corresponding to 200 Gbps, we obtain the curves in Fig. 3(a). From there, we can observe that PAM-4 (light-blue dashed) and PAM-6 (orange solid) have similar TRX bandwidth requirements, with PAM-8 (green dashed-dotted) requiring larger bandwidth. Slightly narrower bandwidths are enough to deliver 200 Gbps in case of PAM-6, which indeed proves to be a potential trade-off solution.

Afterwards, starting from the scenario analyzed in Fig. 3(a), we investigate how the requirements change if we test other levels of RIN, IRND or equalizer type. When the RX bandwidth is larger, also an increase in the amount of generated noise is expected. Thus, if for instance the IRND grows to 20 pA/$\sqrt{\text{Hz}}$ (Fig. 3(b)), the value considered in [4], we observe a remarkable increase of the bandwidth required by both TX an RX to deliver 200 Gbps net rate. In this case, PAM-4 is the less demanding modulation format, as it is more tolerant to noise. Instead, PAM-8 is completely sunk in the noise and it is not able to deliver 200 Gbps, at least for the range of bandwidths considered. At the same time, with the advancement of the technology, a decrease of the generated noise is targeted for the next generation devices. Fig. 3(c) shows the 200 Gbps

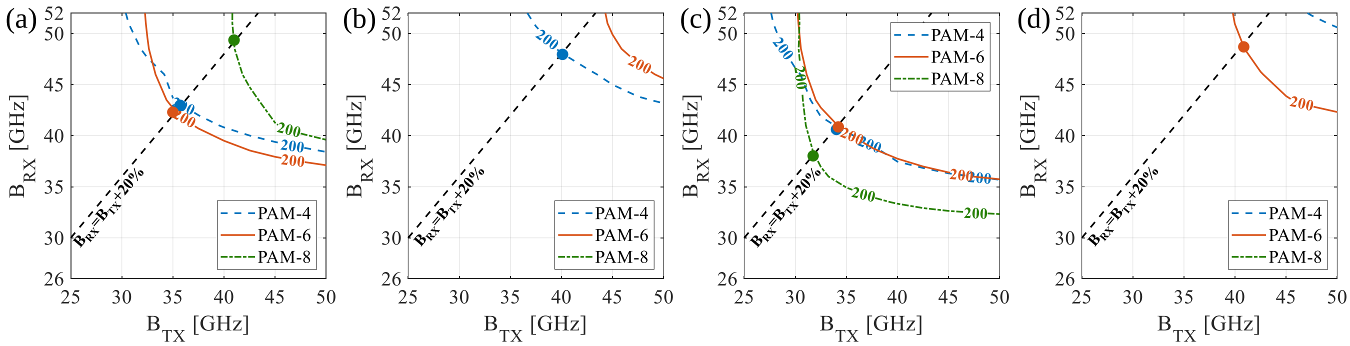

Fig. 3. Bandwidth requirements at 940 nm for all PAM-M modulation formats (light-blue dashed: PAM-4, orange solid: PAM-6, green dashed-dotted: PAM-8) for different scenarios: (a) RIN=-145 dBe/Hz, IRND=14.1 pA/$\sqrt{\text{Hz}}$ and MLSE, (b) RIN=-145 dBe/Hz, IRND=20 pA/$\sqrt{\text{Hz}}$ and MLSE, (c) RIN=-147 dBe/Hz, IRND=14.1 pA/$\sqrt{\text{Hz}}$ and MLSE, and (d) RIN=-145 dBe/Hz, IRND=14.1 pA/$\sqrt{\text{Hz}}$ and FFE.

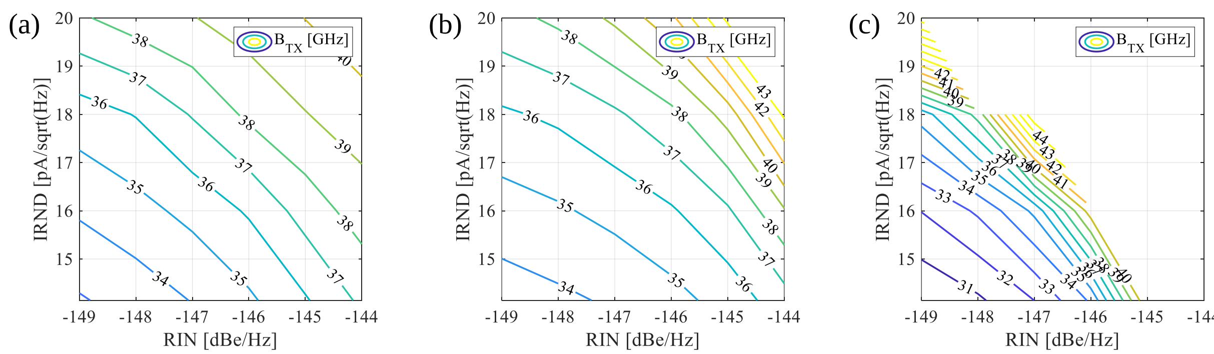

Fig. 4. Requirements of transmitter bandwidth ($\mathrm{B_{TX}}$) as a function of RIN and IRND at 940 nm and MLSE for: (a) PAM-4, (b) PAM-6 and (c) PAM-8. The received bandwidth ($\mathrm{B_{RX}}$) is assumed to be 20% larger than $\mathrm{B_{TX}}$.

TABLE I
SET OF TRX BANDWIDTHS IN THE FORM ($\mathrm{B_{TX}}$,$\mathrm{B_{RX}}$) [GHZ] FOR THE CHANNEL AT 940 nm.

Scenario	PAM-4	PAM-6	PAM-8
RIN=-145 dBe/Hz, IRND=14.1 pA/$\sqrt{\text{Hz}}$, MLSE	(35.8,43.0)	(35.4,42.4)	(41.0,49.2)
RIN=-145 dBe/Hz, IRND=20 pA/$\sqrt{\text{Hz}}$, MLSE	(40.1,48.1)	-	-
RIN=-147 dBe/Hz, IRND=14.1 pA/$\sqrt{\text{Hz}}$, MLSE	(34.1,40.9)	(34.2,41.0)	(31.9,38.2)
RIN=-145 dBe/Hz, IRND=14.1 pA/$\sqrt{\text{Hz}}$, FFE	-	(40.8,48.9)	-

iso-curves assuming that the RIN decreases to -147 dBe/Hz, still for IRND=14.1 pA/$\sqrt{\text{Hz}}$ and MLSE. Being the most tolerant of the three formats to bandwidth limitations and benefiting from a significant reduction in RIN, PAM-8 is now the format requiring the narrowest TRX bandwidth. On the other hand, almost same TRX bandwidths are required by PAM-4 and PAM-6. It is interesting to notice that, especially for PAM-8, the 200 Gbps iso-curve has an asymptotic behavior with respect to $\mathrm{B_{TX}}$ and $\mathrm{B_{RX}}$. This means that, above a certain value, there is not a substantial improvement if a wider bandwidth is considered. Finally, if a less sophisticated equalizer is assumed, such as the FFE (Fig. 3(d)), even larger bandwidths are necessary. Only PAM-6 is able to transmit at 200 Gbps with reasonable TRX bandwidths.

In all analyzed cases, depending on the design and fabrication limitations of TX and RX, we can move on the iso-curves and select the proper set of bandwidths. However, based on the technology advancements, in general it is easier to fabricate TIAs and photodiodes with larger bandwidths than laser sources with larger bandwidths. To further remove one degree of freedom, we assume a fixed relation between $\mathrm{B_{TX}}$ and $\mathrm{B_{RX}}$: $\mathrm{B_{RX}}$ is usually 20% larger than $\mathrm{B_{RX}}$. By intersecting the resulting line with the iso-curves in Fig. 3, we can determine the required TRX bandwidths, when possible. The set of values are reported in Table I.

With this assumption, we can make further investigations on the impact of RIN and IRND in the design of the TRX. In Figs. 4(a)-(c) we illustrate the contour plot of the TX bandwidth varying the RIN and the IRND for PAM-4, PAM-6 and PAM-8, respectively. RIN ranges from -149 dBe/Hz to -144 dBe/Hz, while the IRND from 14.1 pA/$\sqrt{\text{Hz}}$ to 20 pA/$\sqrt{\text{Hz}}$. As expected, we can see that PAM-4 (Fig. 4(a)) is more tolerant to noise than the other two modulation formats. Indeed, for PAM-4, the $\mathrm{B_{TX}}$ ranges from 33 GHz, when the

RIN and the IRND are lower, to ∼40 GHz, when the RIN and the IRND are higher. A similar behavior is observed in case of PAM-6 (Fig. 4(b)). However, compared to PAM-4, larger TX bandwidths with values above 40 GHz are required when RIN and IRND are higher.

The detrimental impact of noise on PAM-8 is clear if we look at Fig. 4(c). PAM-8 becomes advantageous when RIN<-148 dBe/Hz and IRND<16 pA/$\sqrt{\text{Hz}}$, as TX bandwidths between 31 GHz and 35 Ghz are required. Nevertheless, when the noise levels start to grow, the demand of bandwidth increases rapidly.

IV. Conclusions

In this paper, we investigated and defined the TRX bandwidth and noise requirements for three PAM-M formats targeting 200 Gbps transmission per lane over 30 m of emulated OM4 fiber link. The analysis was performed on the worst case channel of the SWDM system, the one operating at 940 nm, which indeed is the most affected by modal dispersion in OM4 fibers. By testing two different equalizers, we showed that a more sophisticated one, such as the MLSE, is essential to design TX and RX with narrower bandwidths, more feasible from a technological and device manufacturing point of view. PAM-4 is more tolerant to higher noise levels than PAM-6 and PAM-8, which instead are more resilient to band limitation thanks to their lower symbol rate.

References

[1] J. Lavrencik, et al., ”4λ × 100Gbps VCSEL PAM-4 transmission over 105m of wide band multimode fiber,” 2017 Optical Fiber Communications Conference and Exhibition (OFC), Los Angeles, CA, USA, 2017, pp. 1-3.

[2] M. V. R. Murty, et al., ”Toward 200G per Lane VCSEL-based Multimode Links,” in Optical Fiber Communication Conference (OFC) 2024, paper M2D.3.

[3] J. M. Castro, et al., “Initial considerations for 100 G VCSEL MMF reaches,” 100 Gb/s Wavelength Short Reach PHYs Study Group Geneva, Switzerland, Jan. 2020.

[4] P. Torres-Ferrera, et al., “Statistical Analysis of 100 Gbps per Wavelength SWDM VCSEL- MMF Data Center Links on a Large Set of OM3 and OM4 Fibers”, Journal of Lightwave Technology, vol. 40, no. 4, pp. 1018–1026, 2022. DOI: 10.1109/JLT.2021.3129455.

[5] A. Zafrany, et al., “A 200Gb/s Low Power DSP-Based Optical Receiver and Transmitter with Integrated TIA and Laser Drivers,” in Optical Fiber Communications Conference and Exhibition (OFC) 2023, paper W2A.2.

[6] M. Hoser, et al., ”Highly Reliable 106 Gb/s PAM-4 850 nm Multi-Mode VCSEL for 800G Ethernet Applications,” 2022 Optical Fiber Communications Conference and Exhibition (OFC), San Diego, CA, USA, 2022, pp. 01-03.

[7] Y. -C. Yang, H. -T. Cheng and C. -H. Wu, “Single-Channel 106.25 Gb/s PAM-4 and 64 Gb/s NRZ Transmission With a 33.4-GHz 850-nm VCSEL With low-RIN Characteristics,” JLT, vol. 42, no. 1, pp. 293-301, 1 Jan.1, 2024, doi: 10.1109/JLT.2023.3306077.

[8] L. Chorchos, “PAM-6 generation using 32-QAM constellation”, in Metro and Data Center Optical Networks and Short-Reach Links II SPIE-OPTO, San Francisco, CA-USA, 2019, pp. 140–149. DOI: 10.1117/12.2509732.